

LGR5 receptor promotes cell-cell adhesion in stem cells and colon cancer cells via the IQGAP1 -Rac1 pathway

Kendra S. Carmon¹, Xing Gong¹, Jing Yi^{1,2}, Ling Wu¹, Anthony Thomas¹,
Catherine M. Moore^{3,4}, Ikuo Masuho⁵, David J. Timson^{3,6}, Kirill A. Martemyanov⁵ and
Qingyun J. Liu^{1,*}

From: ¹The Brown Foundation Institute of Molecular Medicine and Texas Therapeutics Institute, University of Texas Health Science Center at Houston, Houston, TX, USA

²Department of Cancer Biology, University of Texas M.D. Anderson Cancer Center, Houston, TX, USA

³School of Biological Sciences, Queen's University Belfast, Medical Biology Centre, 97 Lisburn Rd., Belfast, BT9 7BL, United Kingdom

⁴Current address: Centre for Infection and Immunity, Division of Clinical Sciences, St George's University of London, Cranmer Terrace, London, SW17 0RE. United Kingdom.

⁵Department of Neuroscience, The Scripps Research Institute Florida, Jupiter, FL 33458, USA

⁶School of Pharmacy and Biomolecular Sciences, University of Brighton, Huxley Building, Lewes Road, Brighton, BN2 4GJ. United Kingdom.

Running title: *LGR5 regulation of cell-cell adhesion*

*To whom correspondence should be addressed to: Qingyun Liu, Brown Foundation Institute of Molecular Medicine, University of Texas Health Science Center at Houston, 1825 Pressler St., Houston, TX 77303, email: Qingyun.liu@uth.tmc.edu; ORCID: 0000-0001-7683-5088.

Key words: stem cells, cell adhesion, LGR5, small GTPase, actin cytoskeleton

Abstract

Leucine rich repeat containing G protein-coupled receptor 5 (LGR5) is a bona fide marker of adult stem cells in several epithelial tissues, most notably in the intestinal crypts and is highly upregulated in many colorectal, hepatocellular, and ovarian cancers. LGR5 activation by R-spondin (RSPO) ligands potentiates Wnt/ β -catenin signaling in vitro, yet deletion of LGR5 in stem cells has little or no effect on Wnt/ β -catenin signaling or cell proliferation in vivo. Remarkably, modulation of LGR5 expression has a major impact on the actin cytoskeletal structure and cell adhesion in the absence of RSPO stimulation, but the molecular mechanism is unclear. Here, we show that LGR5 interacts with IQ motif containing GTPase activating protein 1 (IQGAP1), an effector of Rac1/CDC42 GTPases, in the regulation of actin

cytoskeleton dynamics and cell-cell adhesion. Specifically, LGR5 decreased levels of IQGAP1 phosphorylation at Ser-1441/1443, leading to increased binding of Rac1 to IQGAP1 and thus higher levels of cortical F-actin and enhanced cell-cell adhesion. LGR5 ablation in colon cancer cells and crypt stem cells resulted in loss of cortical F-actin, reduced cell-cell adhesion, and disrupted localization of adhesion-associated proteins. No evidence of LGR5 coupling to any of the four major subtypes of heterotrimeric G proteins was found. These findings suggest that LGR5 primarily functions via the IQGAP1-Rac1 pathway to strengthen cell-cell adhesion in normal adult crypt stem cells and colon cancer cells.

Introduction

LGR5 (leucine-rich repeat containing, G protein-coupled receptor 5) has emerged as an authentic marker of adult stem cells in several epithelial tissues, including the intestine, liver, skin, stomach, and ovarian epithelium (1,2). LGR5 and its closely related homologs, LGR4 and LGR6, consist of a large extracellular domain (ECD) with 17 leucine-rich repeats and a seven-transmembrane (7TM) domain typical of the rhodopsin family of G protein-coupled receptors (GPCRs) (3,4). Several studies have shown that the four R-spondin growth factors (RSPO1-4) can bind to LGR4-6 and potentiate canonical/ β -catenin-dependent Wnt signaling in some cell types (5-7). Although LGR4-6 are homologous to GPCRs and thus classified into this family, their function in modulation of Wnt signaling is independent of heterotrimeric G-proteins (5,6,8). For LGR4, it was shown that RSPO-LGR4 potentiates Wnt signaling by inhibiting the two E3 ubiquitin ligases RNF43 and ZNRF3 which otherwise antagonize Wnt signaling through ubiquitination and subsequent degradation of Wnt receptors (9,10). More recently, we showed that RSPO-LGR4 also functions through the IQGAP1 scaffolding protein to potentiate Wnt signaling via a supercomplex formation with the Wnt receptor complex (11). The interaction of LGR4 with IQGAP1 enhances levels of β -catenin through MEK1/2-mediated phosphorylation of LRP6 and promotes association with cytoskeletal components to regulate focal adhesion (FA) assembly and cell migration (11).

On the other hand, the exact roles and mechanism of LGR5 in the potentiation of Wnt signaling and the regulation of cellular functions remain enigmatic. LGR5 is currently the most recognized marker of adult stem cells in multiple epithelial tissues. Knockout (KO) of LGR5 in the mouse had no effect on Wnt/ β -catenin signaling or the self-renewal of stem cells in the intestine (6,12,13) and liver (14) whereas LGR4 is absolutely essential. On the other hand, overexpression or knockout of LGR5 in several colon and liver cancer cell lines led to significant changes in actin cytoskeleton

structures and cell-cell adhesion in the absence of RSPO stimulation (15,16). Furthermore, overexpression of endocytosis-impaired LGR5 led to the formation of extremely elongated filopodia (also called cytonemes) in HEK293 cells, suggesting robust, RSPO-independent activity in cytoskeleton reorganization as HEK293 cells express little RSPOs endogenously (17). Just recently, it was shown that knocking-in of endocytosis-deficient LGR5 into crypt stem cells resulted in decreased fitness of the stem cells without affecting proliferation (18). Intriguingly, LGR5 was reported to be constitutively coupled to the $G\alpha_{12/13}$ subclass of heterotrimeric G protein in the absence of RSPOs to activate the Rho-GTPase pathway (19). This coupling, however, was neither verified independently nor evaluated in LGR5's role in the regulation of actin-cytoskeleton. Taken together, these findings suggest that LGR5 has an important role in stem cell fitness through the control of actin cytoskeleton and cell adhesion, though the exact mechanisms are yet to be defined.

The mammalian IQGAPs (IQ motif containing GTPase activating proteins) are a group of three related intracellular proteins (IQGAP1-3) with pivotal roles in the regulation of cytoskeletal structure, cell-cell adhesion, polarization, and migration (20-22). IQGAPs integrate signaling crosstalk within the cell through binding to and modulating the activities of a plethora of signaling molecules, including members of the Wnt pathway (APC, β -catenin, E-cadherin), F-actin, MAP kinases, and Rho GTPases (20,22). The Rho family of small GTPases consists of the Rac, Rho, and CDC42 subfamilies which are guanine nucleotide-binding proteins that cycle between an active GTP-bound state and an inactive GDP-bound form to regulate multiple actin dynamics and signaling transduction pathways (23). Even though IQGAP1 contains a GTPase activating protein-like domain, it actually stabilizes GTP binding rather than catalyzes hydrolysis of GTP in Rac1/CDC42 (20-22).

Instead, IQGAP1 binds to the active forms of Rac1 and CDC42 to coordinate actin assembly and control cell-cell adhesion (20,22). Specifically, binding of Rac1/CDC42 to IQGAP1 inhibits the IQGAP1- β -catenin interaction, leading to an increase in membrane-bound β -catenin, cell-cell adhesion and F-actin cross-linking (20,24). Rac1/CDC42 binding to IQGAP1 is inhibited by phosphorylation at two serine sites (Ser-1441 and Ser-1443) of IQGAP1 (25-27). Here we show that LGR5 interacts with IQGAP1 and decreases phosphorylation at these two serine sites, leading to increased binding of Rac1 and consequently enhancement of cell-cell adhesion. Ablation of LGR5 in colon cancer cells and in intestinal crypt stem cells results in a disorganized cytoskeletal structure with loss of cortical F-actin, suggesting an intricate role for the receptor in cancer and for retaining stem cells within the intestinal stem cell niche.

Results

Knockout of LGR5 disrupts the cytoskeletal architecture of intestinal crypt organoids. LGR5 expression is restricted to the crypt stem cells in the intestine, but its conditional knockout was found to have no obvious effect on the proliferation and differentiation of the stem cells both in vivo and ex vivo (6,28). We asked if loss of LGR5 affects cytoskeletal structures of crypt stem cells given the effect of LGR5 on actin-cytoskeleton in cancer cell lines (15,16). Intestinal organoids were generated from LGR5^{-/-} (LGR5-EGFP-IRES-creERT2) homozygotes and their WT (wild-type) littermates and cultured in matrigel as described (29). LGR5 KO was verified by genotyping and positive GFP expression in the stem cells (Fig. 1A). The organoids were passaged 2-3 times and no obvious difference was observed between organoids of LGR5^{-/-} and those of WT in growth and morphology. F-actin staining with rhodamine-phalloidin showed that LGR5^{-/-} organoids had significantly lower levels of cortical F-actin, particularly on the basolateral side of the crypts (Fig. 1B-C).

Additionally, β -catenin was disorganized in LGR5^{-/-} organoids (Fig. 1D-E). In WT organoids, β -catenin was clearly localized to the cytoplasmic membrane, especially at the cell-cell junctions, with some cytoplasmic expression (Fig. 1D). Quantification of the staining indicated that only ~11% of cells in LGR5^{-/-} crypts retained wild-type levels of β -catenin at the cell-cell junction ($p \leq 0.001$) (Fig. 1E). These results suggest that LGR5 is critical for the organization of actin cytoskeletal structures in crypt stem cells and potentially cell-cell adhesion, yet the exact mechanisms involved remain unknown.

Overexpression of LGR5 alters actin cytoskeleton and increases cell-cell adhesion. To understand how LGR5 regulates actin cytoskeleton and cell adhesion, we examined the effect of overexpressing LGR5 in epithelial cell lines. CHO cells stably overexpressing full-length human LGR5 were obtained and receptor expression was analyzed using LGR5-specific antibody. Immunocytochemistry (ICC) analysis showed that LGR5 was located on the cell surface (Fig. 2A, panels a-b). Interestingly, it was apparent that cells overexpressing LGR5 were slightly more rounded, substantially reduced in size, and appeared more adherent and compact (Fig. 2A, panels c-d). These observations paralleled the morphological changes observed in cancer cell lines following LGR5 overexpression (15,16). Quantification of relative cell length showed that CHO-LGR5 cells were shorter when compared to parental CHO cells (Fig. 2B). Phalloidin staining showed an apparent increase in cortical F-actin in CHO-LGR5 cells when compared to parental cells (Fig. 2A, panels e-f). Quantification of the average cortical actin fluorescence intensity per cell indicated a significant increase in intensity in CHO-LGR5 cells ($p \leq 0.001$) (Fig. 2C). We then asked if these LGR5-induced changes involve RSPO ligands. RT-PCR analysis showed that parental and CHO-LGR5 cell lines did not express any of the four RSPOs (Supplementary Fig. S1),

indicating that LGR5 has constitutive or RSPO-independent activity in regulating actin-cytoskeleton and cell morphology.

Given the changes induced by LGR5 in the actin cytoskeleton, the effects of LGR5 on cell migration and adhesion were also determined. CHO-LGR5 cells showed significant reduction in cell migration using the wound-healing assay (Fig. 2D). In the Calcein-AM-based cell-cell adhesion assay which measures the retention of a fluorescent dye in cells attached to other cells without the dye (30), CHO-LGR5 cells exhibited significantly stronger adhesion compared to parental CHO cells (Fig. 2E).

Previously, we reported the generation and characterization of HEK293T cells stably expressing vector, LGR5-WT, and LGR5- Δ C (endocytosis impaired due to the deletion of the C-terminal tail sequence AA837-907) in the regulation of Wnt/ β -catenin signaling (31). Our findings showed that the C-terminal tail of LGR5 is not only important for internalization, but also critical for regulating receptor signaling. Snyder et al reported that overexpression of an endocytosis-impaired LGR5 mutant with a truncated C-terminal tail led to formation of cytonemes in HEK293 cells, whereas LGR5 wild-type (WT) displayed few to no such cellular protrusions (32). Furthermore, the same LGR5 mutant was recently shown to reduce stem cell fitness in vivo by lineage tracing (18). Here, we examined the effect of Myc-tagged LGR5-WT and - Δ C overexpression on the actin cytoskeleton and cell adhesion. F-actin staining showed that cells overexpressing LGR5 displayed more compact structure and increased levels of F-actin at cell-cell contacts (Fig. 3A), which were confirmed by quantification (Fig. 3B). Cells expressing LGR5- Δ C, however, displayed cytoneme-like structures without increased levels of F-actin at the cell-cell contacts (Fig. 3A-B), consistent with the findings of Snyder et al. (32). F- and G-actin were then extracted from the three cell lines and their relative level was determined by immunoblot analysis and quantified (Fig. 3C-D). Cells overexpressing LGR5-WT

showed higher ratio of F- to G- actin when compared to vector and LGR5- Δ C cells. Of note, HEK293 cells express RSPOs at very low levels as shown by RT-qPCR (17), and are highly sensitive to RSPO stimulation in Wnt/ β -catenin signaling (5,6,8), suggesting that LGR5-induced actin-cytoskeleton changes are RSPO-independent. Indeed, treatment with RSPO1 overnight had no significant effect on F/G actin ratio either in control or LGR5 cells (Fig. 3E-F), confirming that the activity is RSPO-independent. Overall, these effects of LGR5 on F-actin structure and cell adhesion in CHO and HEK293 cells are similar to the phenotypes observed with overexpression of LGR5 in colon and liver cancer cell lines (15,16). Importantly, the effect of LGR5 on the actin cytoskeleton were all displayed in the absence of RSPO stimulation (either endogenous or exogenous), indicating that these activities do not involve the two E3 ligases RNF43/ZNRF3.

LGR5 is not coupled to heterotrimeric G proteins. Next, we attempted to identify intracellular mechanism that may mediate the effect of LGR5 on the actin-cytoskeleton and cell adhesion. Previously, we and others showed that LGR5 is not coupled to any of the three types of heterotrimeric G proteins that give rise to secondary messenger formation (cAMP or Ca²⁺) or to β -arrestin in response to RSPO stimulation (5,6,8). Intriguingly, Kwon et al reported that LGR5 coupled to the G $\alpha_{12/13}$ -Rho GTPase pathway to activate the SRF-RE (serum response factor-response element) pathway in the absence of RSPO stimulation (19). However, neither binding nor direct activation of G $\alpha_{12/13}$ (exchange of GDP for GTP) by LGR5 was demonstrated (19). As the G $\alpha_{12/13}$ pathway plays a critical role in the control of actin dynamics and cell migration, we examined if LGR5 activates G $\alpha_{12/13}$ or any of the other heterotrimeric G protein subclasses using a direct method. Activation of heterotrimeric G-proteins by 7TM receptors can be monitored directly by highly sensitive assays based on changes in Bioluminescence Resonance Energy Transfer (BRET, Fig. 4A) that is dependent

on the release of the G $\beta\gamma$ subunit from the activated GPCR and its subsequent binding to a fragment of GRK3 (33-35). Using this assay, we tested if LGR5 increases guanine nucleotide exchange factor (GEF) activity of any of the four major subtypes of heterotrimeric G proteins (Gas, Gai/o, G α_q , and G $\alpha_{12/13}$) with RSPO stimulation. No significant signal by LGR5 was detected with any of the four G proteins that were tested (Fig. 4B-E), whereas all positive control receptors showed robust activity (Fig. 4B-E). We then performed a GTPase pulldown assay to measure activation of RhoA (which occurs downstream of G $\alpha_{12/13}$) in HEK293 cell lines stably overexpressing vector, LGR5, or GPR56, a GPCR known to activate the G $\alpha_{12/13}$ /RhoA signaling pathway constitutively (36). Our results showed that GPR56 increased active RhoA levels with or without serum stimulation compared to vector cells, whereas LGR5 caused a slight decrease (not significant) in the level of Rho-GTP (Fig. 4F-G). Based on these results, we conclude that LGR5 does not appear to bind to or function through G $\alpha_{12/13}$ and further confirmed that LGR5 is not coupled to the other three subclasses of heterotrimeric G proteins.

LGR5 interacts with IQGAP1. LGR4 was found to interact with the intracellular scaffold protein IQGAP1 to potentiate Wnt signaling and regulates focal adhesion formation and cell migration (11). IQGAP1 plays a major role in the control of actin cytoskeleton and cell adhesion and migration, largely through modulation of the small G protein Rac1 and CDC42 (37,38). Given the homology of LGR4 and LGR5 and that IQGAP1 and IQGAP3 appeared as proteins that co-purified with both receptors in mass spectrometry analysis (6), we tested if LGR5 also interacts with IQGAP1. Using recombinant overexpression and co-IP analysis in HEK293T cells, we found that Flag-IQGAP1 did interact with Myc-tagged LGR5-WT as well as with the C-terminal tail truncated mutant LGR5- Δ C (31) (Fig. 5A). As a negative control, we show that IQGAP1 did not pull down with Myc-tagged LGR5-ECD anchored to the membrane with

a single transmembrane domain (Fig. 5A). These results indicate that IQGAP1 binds to the 7TM domain of LGR5 and this interaction does not require the C-terminal tail (AA837-907). To verify that this interaction is not due to overexpression, co-IP analysis was carried out with the LoVo colon cancer cell line, which has high endogenous levels of LGR5 (39). Indeed, endogenous IQGAP1 in LoVo cells was pulled down using an LGR5-specific antibody (Fig. 5B). To map the IQGAP1 domains that interact with LGR5, we utilized a series of Flag-IQGAP1 truncation and deletion mutants (Fig. 5C). Co-IP studies demonstrated that LGR5 binds to the C-terminal half of IQGAP1 spanning amino acids 893-1657 (Fig. 5C-E). Unlike LGR4 (11), however, we detected weak binding of LGR5 to the GRD domain, yet strong binding to a variant lacking the GRD domain (Δ GRD) (Fig. 5D-E). We then tested if LGR5 could bind to a purified IQGAP1 fragment spanning amino acids 877-1558 (DR6 or GRDD1-RGCT) that was expressed in *E.coli*, purified and shown to bind to CDC42 (26). LGR5-WT, but not LGR5-ECD, pulled down DR6 (Fig. 5F). Overall, these results suggest that the 7TM domain of LGR5 interacts with the C-terminal portion of IQGAP1, although the exact motifs from each partner are yet to be mapped.

LGR5 decreases phosphorylation of IQGAP1 to enhance IQGAP1-Rac1 interaction. IQGAP1 regulates the actin cytoskeleton by functioning as an effector of CDC42 or Rac1 (37). We examined if LGR5 affects the binding of IQGAP1 to CDC42, Rac1, or both. Using co-IP analysis, we found that Rac1, but not CDC42 or RhoA, was pulled down with IQGAP1 in CHO-LGR5 cells (Fig. 6A-B). In contrast, we did not detect any of the Rho GTPases being associated with IQGAP1 in control CHO cells under the same conditions (Fig. 6A-B). Furthermore, actin consistently co-precipitated with IQGAP1 in CHO-LGR5 cells but was not detectable in parental CHO cells (Fig. 6A). We then tested whether the levels of total “free”

active Rac1 (i.e. not bound to IQGAP1) was altered due to LGR5 overexpression using a GST-PBD (PAK1) pull-down assay. Of note, IQGAP1 binds active GTPases with higher affinity and different specificity than PAK1 PBD (40). The PBD-bound active Rac1 levels were equivalent for each cell line (Fig. 6C), suggesting that LGR5 may stabilize the binding of Rac1 to IQGAP1 without affecting the overall levels of “free” active Rac1. In addition, LGR5-mediated binding of Rac1/actin to IQGAP1 was not affected by RSPO treatment (Supplementary Fig. S2A.), again suggesting that the effect of LGR5 on actin-cytoskeleton is independent of RSPO stimulation.

Binding of Rac1/CDC42 to IQGAP1 is regulated by phosphorylation of IQGAP1 at two sites (Ser-1441 and -1443) (25,26,41). Detailed kinetic analysis showed that phosphorylation at Ser-1443 led to decrease in the affinity of human IQGAP1 for Rac1 and CDC42 (27). To test if LGR5 regulates IQGAP1-Rac1 interaction through modulation of IQGAP1 phosphorylation, we probed the level of phospho-IQGAP1 with an anti-phosphoserine antibody (no antibody specifically against Ser-1441 or Ser-1443 of IQGAP1 is available (42)). Overexpression of LGR5-WT in HEK293 cells led to drastic decrease in the level of phospho-Ser (pSer) of IQGAP1 when compared to vector cells (Fig. 6D). Remarkably, LGR5- Δ C which does not increase cortical F-actin, did not alter the levels of pSer of IQGAP1 (Fig. 6D). Follow-up co-IP analysis confirmed that IQGAP1 showed increased binding to actin and Rac1 in HEK293 cells (Fig. 6E). To examine if the decreased level of pSer of IQGAP1 in LGR5 cells is due to inhibition of phosphorylation or enhancement of dephosphorylation, LGR5 and vector cells were treated with PMA for 10 min which induces IQGAP1 phosphorylation at Ser-1441/1443 and their pSer levels of IQGAP1 were compared. As shown in Fig. 6F, no difference was seen between LGR5 and vector in response to PMA treatment, suggesting that LGR5 did not inhibit acute

phosphorylation of IQGAP1 by PKC. To confirm that the detected phospho-IQGAP1 signal was specific for Ser-1441/-1443 phosphorylation, we generated an IQGAP1 mutant with both serines changed to alanine (SKS \rightarrow AKA). As shown by IP in Supplementary Fig. S2B, no signal was detected with the mutant IQGAP1 while IQGAP1-WT showed a strong signal following PMA treatment. These results suggest that LGR5-induced decrease in IQGAP1 phosphorylation at Ser-1441/-1443 was probably due to increased dephosphorylation.

Knockdown of LGR5 in colon cancer cells leads to loss of IQGAP1-associated Rac1/actin and disruption of cytoskeletal structure. The LoVo colon cancer cell line is mutated in the tumor suppressor and Wnt inhibitor APC and expresses high levels of LGR5 and IQGAP1 (39). Microarray data of this cell line in the CCLE database showed no expression of RSPOs (43), which we confirmed by RT-qPCR analysis. LoVo cell lines stably expressing two independent LGR5 shRNA constructs, shLGR5-86 and shLGR5-89, along with vector control were generated. Both shRNA constructs yielded \geq 90% reduction in LGR5 as verified by WB and ICC (Fig. 7A-B, top panel). A LoVo cell line stably expressing an IQGAP1 shRNA (shIQGAP1-85) which we used previously in lung cancer cell lines (11), was also generated and loss of IQGAP1 was confirmed by WB (Fig. 7A).

We first examined F-actin structures in these cell lines and found that, strikingly, shIQGAP1, shLGR5-86, and shLGR5-89 cell lines all displayed a significant loss of cortical F-actin and showed an overall disorganized cytoskeletal structure when compared to control cell lines (Fig. 7B, lower panels). Correspondingly, loss of LGR5 expression resulted in reduced levels of IQGAP1 localized to the plasma membrane at cell-cell adhesion sites (Fig. 7C-D). Using ICC, we also analyzed E-cadherin and β -catenin, which are critical to the formation and stabilization of cell-cell adhesion (24). Loss of LGR5 or IQGAP1 resulted in decreased membrane-

associated β -catenin accompanied by increased β -catenin levels in the cytoplasm (Fig. 7E-F), which was also confirmed by WB (Fig. 7A, lower panel). However, we did not observe any obvious changes in the level of E-cadherin or its localization (Supplementary Fig. S3). These results suggest that LGR5-IQGAP1 functions to regulate β -catenin localization and is essential for the formation and/or stabilization of cortical F-actin.

Formation of stable E-cadherin-mediated cell-cell adhesion depends on cortical F-actin which is connected to the adhesion complex via α -catenin (44). The loss of cortical F-actin in LGR5 and IQGAP1 KD cells suggests that loss of LGR5-IQGAP1 interaction may decrease cell-cell adhesion. Using the Calcein-AM fluorescence-based cell-cell adhesion assay, we demonstrated that KD of LGR5 resulted in a reduction in cell-cell adhesion (Fig. 8A). Poorly organized cortical F-actin is also expected to have increased levels of soluble E-cadherin (45). Indeed, we found that LoVo cells lacking LGR5 showed significant increase in the ratio of soluble vs insoluble E-cadherin when extracted by NP-40 (Fig. 8B-C).

As overexpression of LGR5-WT led to decrease in phosphorylation of Ser-1441/1443 of IQGAP1 and consequently increased Rac1 binding to IQGAP1, we tested if the opposite was true in LoVo cells with KD of LGR5. Co-IP was performed with an anti-IQGAP1 antibody to pull-down endogenous IQGAP1 in parental, vector, and shLGR5-89 cells (shIQGAP1 cells were included as a negative control for IQGAP1 antibody specificity) (Fig. 8D). As expected, we found that KD of LGR5 resulted in loss of Rac1 and actin association with IQGAP1 (Fig. 8D). Furthermore, the level of IQGAP1 phosphorylation was found to be higher in LGR5 KD cells (Fig. 8E). Together with the LGR5 overexpression data, these findings coherently suggest a mechanism where LGR5 reduced phosphorylation of IQGAP1 at Ser-1441/1443 to increase the IQGAP1-Rac1 interaction and ultimately enhance

cell-cell adhesion via regulating the actin cytoskeleton.

Discussion

LGR5 is currently the most widely recognized and utilized stem cell marker in the gastrointestinal tract and several other epithelial tissues and it is upregulated in a substantial fraction of solid tumors (1,2). However, the exact roles and mechanisms of LGR5 in normal adult stem cells and cancer cells remain poorly defined. Notably, expression of LGR5 is not essential for the survival of crypt stem cells in vivo or ex vivo (6,28). The function of LGR5 in cancer cells appeared to be tumor-type dependent, with tumor suppressor-like activity in colon and liver cancer cells and tumor-promoting activity in other cancer cell types (15,16,46). Mechanistically, multiple studies showed that LGR5 can bind the RSPO1-4 family of stem cell factors to potentiate Wnt/ β -catenin signaling in HEK293T cells (5,6,8). RSPOs (with the exception of RSPO4) also bind to the two E3 ligases RNF43/ZNFR3 which ubiquitinate Wnt receptors for degradation and the co-crystal structure of LGR5-RNF43-RSPO had been solved (47,48). Based on these studies the current model is that LGR5, like LGR4, functions as a high-affinity co-receptor of RSPOs facilitating the binding of RSPOs to inhibit RNF3/ZNRF3, leading to enhanced Wnt signaling (49). However, direct evidence of RSPO-LGR5 mediating the inhibition of RNF43/ZNRF3 has never been reported. Furthermore, KO of LGR5 in multiple tissues led to increase in levels of Axin2 (marker of Wnt/ β -catenin signaling), suggesting that LGR5 does not play a major, positive role in Wnt/ β -catenin signaling in stem cells in vivo (12-14). Remarkably, a consistent finding is that LGR5 overexpression in cancer cells alters actin cytoskeleton structure and increases cell-cell adhesion in the absence of endogenous or exogenous RSPO stimulation (15,16). Such LGR5-induced changes in actin-cytoskeleton are unlikely mediated by inhibition of RNF43/ZNRF3 since these changes occur in the absence

of RSPOs which are essential for interacting with RNF43/ZNRF3. Here we present evidence for a novel mechanism where LGR5 is coupled to the intracellular scaffold signaling protein IQGAP1 to regulate the actin cytoskeleton and cell-cell adhesion.

IQGAP1 interacts with a plethora of receptors and effectors to coordinate signaling and regulate actin cytoskeleton dynamics. We found that LGR4 interacts with the GRD domain of IQGAP1 to potentiate both the canonical and non-canonical pathways of Wnt signaling (11). In comparison, LGR5 interacts not only with the GRD domain but also with a C-terminal domain of IQGAP1. Interestingly, overexpression of LGR4 and LGR5 have opposite effect on the actin cytoskeleton and cell adhesion and migration (11,15,16,50,51). The distinctive domains of IQGAP1 involved in binding to LGR5 may underlie the differential effect of LGR4 and LGR5 on these cellular processes and morphology. The 7TM domains between LGR4 and LGR5 are highly conserved whereas their C-terminal tails are quite divergent. LGR5 lacking its C-terminal tail is endocytosis-impaired, potentiates Wnt/ β -catenin signaling (31,52), and induces the formation of cytonemes in HEK293 similar to those induced by full length LGR4 (32). These findings imply that the C-terminal tail of LGR5, although not essential for IQGAP1 binding, may interact with additional domains on IQGAP1 or other proteins bound to IQGAP1 to exert effects distinct from those of LGR4. As LGR5 does not appear to affect acute phosphorylation of IQGAP1, a potential mechanism is that the C-terminal tail of LGR5 recruits a Ser/Thr phosphatase to dephosphorylate IQGAP1.

Initially, we found that overexpression of LGR5 consistently led to increased binding of Rac1 and actin to IQGAP1 in co-IP analysis. Since it was reported that binding of Rac1/CDC42 to IQGAP1 is inhibited by phosphorylation at Ser-1441/1443 of IQGAP1 (26,27,41), we asked if LGR5 modulates phosphorylation of IQGAP1 at these sites to regulate IQGAP1-Rac1 interaction. Indeed, LGR5

overexpression and KD of LGR5 led to a significant decrease and increase in Ser-1441/1443 phosphorylation, respectively, and LGR5 had no effect on PMA-induced phosphorylation of IQGAP1. Furthermore, overexpression of LGR5- Δ C which induced cytoneme formation without increase in total F-actin, had no effect on phosphorylation (Fig. 5D). These results suggest that the C-terminal tail of LGR5 regulates phosphorylation of the two serine sites, potentially through recruitment of phosphatase(s). In turn, decreased levels of phosphorylated IQGAP1 at Ser-1441/1443 lead to increased Rac1 binding to IQGAP1. Importantly, Rac1-bound IQGAP1 can no longer interact with β -catenin, yet can still bind to and crosslink F-actin filaments (20), leading to an increase in E-cadherin- β -catenin- α -catenin complex formation and F-actin crosslinking, and therefore stronger cell-cell adhesion (20,24). Thus, we propose a model whereby LGR5-induced depletion of IQGAP1 phosphorylation is increases the IQGAP1-Rac1 interaction with concomitant loss of IQGAP1- β -catenin interaction, eventually leading to strengthening of cell-cell adhesion (Fig. 9). Furthermore, the slight increase of Wnt/ β -catenin signaling in LGR5 KO tissues (12-14) may be explained by release of β -catenin from adherens junction sites at the plasma membrane in LGR5 KO cells with weakened cell-cell adhesion (53).

The critical role of LGR5 in the control of cell-cell adhesion may also shed light on reasons why LGR5 is specifically expressed by adult stem cells in various epithelial tissues. Stem cell niches provide an adhesive milieu that can selectively retain daughter stem cells, but not differentiated daughter cells (54). In the small intestine, LGR5⁺ stem cells (~14 cells per crypt) are interspersed with Paneth cells throughout the base of the crypt or stem cell niche (55). In vivo imaging has shown that LGR5⁺ stem cells located at the crypt base experience a survival advantage over border stem cells that can be passively displaced into the transit-amplifying region along the sides of the crypt (56). It is thus

tempting to speculate that the stem cells that form stronger cell-cell adhesion contacts have a competitive advantage in terms of being retained in the niche and remaining as stem cells. Given that LGR5 is not essential for the growth and survival of crypt stem cells, it is conceivable that the receptor may primarily function to promote strong cell-cell adhesion in stem cells, which, in turn, retains these cells within the crypt base to maintain homeostasis in the intestinal epithelium. Indeed, a recent paper showed that intestinal stem cells expressing LGR5 without its C-terminal tail were less “fit” in vivo as manifested by their decreased life-span in the intestine (18). This is consistent with our model that LGR5 lacking the C-terminal can not reduce phosphorylation of IQGAP1, leading to lower level of Rac1 binding and decrease in cell-cell adhesion, and thus faster elimination in vivo.

EXPERIMENTAL PROCEDURES

Plasmids and cloning. Plasmids encoding Myc-LGR5, Myc-LGR5-ECDTM, Myc-LGR5 Δ C, and all Flag-tagged mouse IQGAP1 deletion/truncation mutants were generated as previously described (5,11). Myc-tagged full-length human GPR56 was cloned into pIRESpuro3 using standard PCR-based methods. FLAG-tagged mouse IQGAP1-CT truncation mutant was constructed by amplifying the fragment containing aa962-1657 from mouse IQGAP1 pCMV-sport6 (Addgene). The PCR product was subcloned into a pcDNA3.1 vector modified to incorporate an N-terminal FLAG-tag. GST-PBD (PAK1) was a gift from Dr. Jeffrey Frost (UT Health Science Center-Houston). The heterotrimeric G protein activation plasmids were described previously (33).

Recombinant proteins, antibodies, and chemicals. Recombinant human RSPO1 was purchased from R&D Systems. IQGAP1 DR6 recombinant protein was produced and purified from E.coli as previously reported (26). For crypt organoid cultures, Noggin was purchased from Peprotech, N-Acetylcysteine was from

Sigma, and N2, B27, and mEGF were all purchased from Life Technologies. All commercial antibodies were used in accordance to manufacturer’s guidelines. For western blot analysis: anti-LGR5 (Abcam ab75732), anti-Rac1 (BD Biosciences #610650), anti-IQGAP1 (BD Bioscience #610611), anti-Flag (Sigma #F7425), anti-G α 13 (Santa Cruz sc-410), Cell Signaling antibodies- anti-CDC42 (#2466), anti-Rho (#8789), anti-Myc (#2272 or #2278), anti- β -catenin (#9562), anti-E-cadherin (#3195), anti- Phospho-(Ser) PKC Substrate Antibody(#2261), and anti- β -actin (#4970). Specificities of all antibodies were confirmed based on protein size and correlation with recombinant expression. For ICC experiments: anti- β -catenin-Alexa 488 (Cell Signaling #2849), anti-E-cadherin-Alexa 488 (Cell Signaling #3199), anti-IQGAP1 (Bethyl #A301), anti-LGR5 (BD Biosciences #562731), and anti-Myc-Cy3 (Sigma #C6594). TO-PRO-3, rhodamine-phalloidin, and rabbit anti-rat Alexa 488 and goat anti-rabbit 488 secondary antibodies were purchased from Life Technologies.

Cell culture and shRNA stable cell line generation. HEK293T and CHO-K1 cells were purchased from ATCC. HEK293T and CHO-K1 cells were cultured in high-glucose DMEM and F-12/HAMs media, respectively, and supplemented with 10% fetal bovine serum (FBS) and penicillin/streptomycin (pen/strep) at 37 °C with 95% humidity/5% CO₂. CHO-LGR5 cells were purchased from DiscoverRx and maintained in F-12/HAMs supplemented with 10% FBS, 300 μ g/ml hygromycin, 800 μ g/ml geneticin, and pen/strep. LoVo cells were obtained from the laboratory of Dr. Shao-Cong Sun at M.D. Anderson Cancer Center, Houston, USA, and maintained in RPMI with 10% FBS and pen/strep. To generate stable KD of LGR5 or IQGAP1, LoVo cells were infected with lentivirus particles produced by co-transfecting HEK293T cells with a pLKO.1 vector incorporating either the LGR5- or IQGAP1- targeted shRNA and packaging plasmids, psPAX2 and pMD2.G, using the Fugene 6 (Roche). Viral infected cells were selected with puromycin. The

shRNA clones were from GE Dharmacon with clone numbers as follows: human LGR5, TRCN0000011586 (shLGR5-86), human LGR5, TRCN0000011589 (shLGR5-89), human IQGAP1, TRCN0000047485 (shIQGAP1-85). The corresponding sequences can be accessed on the GE Dharmacon website <http://dharmacon.gelifesciences.com>.

Intestinal crypt organoid culture. All animal experiments were performed in accordance with a protocol approved by the Animal Protocol Review Committee of the University of Texas Health Science Center at Houston. B6.129P2-LGR5^{tm1(cre/ERT2)Cle/J} mice were purchased from Jackson Labs and bred to produce wild-type and LGR5 knockout (KO) mutant offspring. Since LGR5 KOs are perinatal lethal, pups were sacrificed and intestines were collected immediately after birth. Tail genotyping was conducted following the standard PCR protocol provided by the Jackson Laboratory. Mouse intestinal crypt organoid cultures were established as previously published (29). Briefly, small intestines were harvested and washed to remove contaminants and villi. Intestinal fragments were incubated in EDTA for 30 min, strained, and pelleted. Crypts were resuspended in matrigel with DMEM/F12 media containing 10mM HEPES, Glutamax, 1X B27, 1X N2, 1mM N-acetylcysteine, 50 ng/ml mEGF, 100 ng/ml mNoggin, 20 ng/ml RSPO1 and Pen/Strep. The media was replenished every 2-3 days and the crypt organoids were mechanically broken down by glass pipette and passaged every 5-6 days.

RT-PCR. Total RNA was extracted by lysing the cells with TRIzol (Life Technologies), followed by the successive addition of chloroform and isopropanol for phase separation and RNA precipitation, respectively. Samples were run through RNeasy Mini Kit columns (Qiagen) according to the manufacturer's protocol, eluted with RNase-free water and DNase treated. cDNA was produced using the iScript kit (BioRad).

Western blot and immunoprecipitation, Heterotrimeric G protein BRET assays were performed as described before (35). Rho-GTP pulldown was carried out using an assay kit (Cytoskeleton, #BK036). F/G actin were separated and extracted using the Triton X-100 assay essential as described previously (57). Quantification of soluble vs insoluble E-cadherin was performed as described before (45). For WB analysis, cells were lysed with RIPA buffer (50 mM Tris-Cl pH 7.4, 150 mM NaCl, 1 mM DTT, 1% Triton X-100, 1% sodium deoxycholate, 0.1% SDS) or GTPase Buffer (25 mM Tris 7.5, 30 mM MgCl₂, 0.13 M NaCl, 0.5% NP-40) for experiments involving GTPase activity. Both buffers were supplemented with protease and phosphatase inhibitors. HRP-labeled secondary antibodies (Cell Signaling) were utilized for detection along with the standard ECL protocol. For co-immunoprecipitation experiments, cell lysates were incubated ~3-4 hrs at 4°C with anti-Myc magnetic beads (Cell Signaling), anti-Flag magnetic beads (Sigma), or glutathione magnetic beads (Sigma), or primary antibody and protein A/G agarose beads (Santa Cruz). Precipitates were washed with lysis buffer followed by PBS and boiled with 2xSDS sample buffer prior to loading for SDS-PAGE and western blot analysis. G protein BRET assays were carried out as describe previously (33). All ligand treatments were performed with Wnt3aCM (diluted 1:5) and 30 ng/ml RSPO, unless otherwise stated. All experiments were performed at least three times.

Immunocytochemistry and Confocal Microscopy. For immunocytochemistry (ICC), CHO and LoVo cell lines were reseeded into 8-well chamber slides (BD Biosciences) and allowed to adhere overnight. Cells were then washed, fixed with 4% paraformaldehyde for 15 min, and permeabilized with 0.1% saponin for 10 min. Cells were incubated with indicated antibodies for 1 hr, rhodamine-phalloidin for 20 min, and TO-PRO-3 nuclear counterstain for 5 min. For ICC of intestinal crypt organoids, organoids were collected, fixed for 30 min and washed from residual

matrigel. Permeabilization and staining were performed in 0.2 ml tubes. Organoids were mounted onto slides using Vectashield (Vector Labs). Confocal microscopy images were collected and analyzed using the Leica TSC SP5 system and LAS AF Lite software. All experiments were performed at least three times.

Wound and cell-cell adhesion assays. For the wound healing assays, CHO or LoVo cells were plated in 12-well plates, grown to near confluency, and started in serum-free media O/N. The next day cells were scratched and serum-free media was replaced with 10% serum. Wound closure was observed over a 12-20 hr period and images were captured and quantified using ImageJ (58). Cell-cell adhesion assays were performed by resuspending CHO or LoVo cells in serum free medium and incubated with 5 μ M Calcein-AM dye for 30 min at 37 °C. After incubation, non-incorporated Calcein-AM was removed by three washes with serum free medium. 1×10^4 of the Calcein-AM-labeled cells were added to a confluent monolayer of CHO or LoVo cells grown in a 96-well plate. After 1 hr (LoVo) or 2 hr (CHO) incubation at 37 °C, non-adherent Calcein-AM-labeled cells were removed by washing with PBS. Relative

fluorescence intensity of the adherent Calcein-AM-labeled cells was measured using a Tecan M1000 plate reader with excitation wavelength of 485 nm and an emission wavelength of 530 nm. All experiments were performed at least three times with triplicates or quadruplicate in each experiment. Data were analyzed using the software GraphPad Prism.

Quantification and Statistical analyses. All quantification of western blot and confocal images were performed using ImageJ (58) to measure integrated density or relative length (CHO cells). Cortical actin was quantified by averaging the integrated density/pixel across 5 pixel length (n \approx 20 cells or crypts). For Lovo cells, IQGAP1 and β -catenin was quantified by measuring the integrated density of membrane and cytoplasm, respectively (n=20-30 cells for each cell line). For each organoid type, the number of cells with wild-type junctional β -catenin expression were counted for the first 20 cells of each crypt starting at the base, averaged, and presented as a percentage (n=15-20 crypts). Student's T-test and ANOVA were performed using GraphPad Prism.

Acknowledgements: We would like to thank Dr. Jeff Frost of UT Health Science Center-Houston for GST-PBD (PAK1) plasmid, Dr. Shao-Cong Sun of M.D. Anderson Cancer Center for providing the LoVo cell line. This work was supported in part by the Cancer Prevention and Research Institute of Texas (CPRIT, RP100678), the US National Institute of Health-NIH (R01GM102485), The Texas Emerging Technology Fund, and the Janice D. Gordon endowment for bowel cancer research (to Q.J.L), the Biotechnology and Biological Sciences Research Council (BBSRC, UK; BB/D000394/1) and Action Cancer (Northern Ireland, UK; PG2 2005) (to D.J.T), and MH105482 (to K.L.M).

Conflict of Interest: QJL is a co-founder of Wntrix. It does not present any conflict of interest with the results described in the present paper.

Author Contribution: Kendra Carmon, Xing Gong, Jing Yi, Ling Wu, Anthony Thomas, Catherine Moore, Ikuo Masuho, David Timson, Kirill Martemyanov and Qingyun Liu acquired and analyzed data. Kendra Carmon and Qingyun Liu conceived and designed the study and wrote the manuscript.

References

1. Barker, N., and Clevers, H. (2010) Leucine-rich repeat-containing G-protein-coupled receptors as markers of adult stem cells. *Gastroenterology* **138**, 1681-1696
2. Koo, B. K., and Clevers, H. (2014) Stem cells marked by the R-spondin receptor LGR5. *Gastroenterology* **147**, 289-302
3. McDonald, T., Wang, R., Bailey, W., Xie, G., Chen, F., Caskey, C. T., and Liu, Q. (1998) Identification and cloning of an orphan G protein-coupled receptor of the glycoprotein hormone receptor subfamily. *Biochem Biophys Res Commun* **247**, 266-270
4. Carter, R. L., Fricks, I. P., Barrett, M. O., Burianek, L. E., Zhou, Y., Ko, H., Das, A., Jacobson, K. A., Lazarowski, E. R., and Harden, T. K. (2009) Quantification of Gi-mediated inhibition of adenylyl cyclase activity reveals that UDP is a potent agonist of the human P2Y14 receptor. *Mol Pharmacol* **76**, 1341-1348
5. Carmon, K. S., Gong, X., Lin, Q., Thomas, A., and Liu, Q. (2011) R-spondins function as ligands of the orphan receptors LGR4 and LGR5 to regulate Wnt/beta-catenin signaling. *Proc Natl Acad Sci U S A* **108**, 11452-11457
6. de Lau, W., Barker, N., Low, T. Y., Koo, B. K., Li, V. S., Teunissen, H., Kujala, P., Haegebarth, A., Peters, P. J., van de Wetering, M., Stange, D. E., van Es, J. E., Guardavaccaro, D., Schasfoort, R. B., Mohri, Y., Nishimori, K., Mohammed, S., Heck, A. J., and Clevers, H. (2011) Lgr5 homologues associate with Wnt receptors and mediate R-spondin signalling. *Nature* **476**, 293-297
7. Glatt, S., Halbauer, D., Heindl, S., Wernitznig, A., Kozina, D., Su, K. C., Puri, C., Garin-Chesa, P., and Sommergruber, W. (2008) hGPR87 contributes to viability of human tumor cells. *Int J Cancer* **122**, 2008-2016
8. Ruffner, H., Sprunger, J., Charlat, O., Leighton-Davies, J., Grosshans, B., Salathe, A., Zietzling, S., Beck, V., Therier, M., Isken, A., Xie, Y., Zhang, Y., Hao, H., Shi, X., Liu, D., Song, Q., Clay, I., Hintzen, G., Tchorz, J., Bouchez, L. C., Michaud, G., Finan, P., Myer, V. E., Bouwmeester, T., Porter, J., Hild, M., Bassilana, F., Parker, C. N., and Cong, F. (2012) R-Spondin potentiates Wnt/beta-catenin signaling through orphan receptors LGR4 and LGR5. *PLoS One* **7**, e40976
9. Hao, H. X., Xie, Y., Zhang, Y., Charlat, O., Oster, E., Avello, M., Lei, H., Mickanin, C., Liu, D., Ruffner, H., Mao, X., Ma, Q., Zamponi, R., Bouwmeester, T., Finan, P. M., Kirschner, M. W., Porter, J. A., Serluca, F. C., and Cong, F. (2012) ZNRF3 promotes Wnt receptor turnover in an R-spondin-sensitive manner. *Nature* **485**, 195-200
10. Koo, B. K., Spit, M., Jordens, I., Low, T. Y., Stange, D. E., van de Wetering, M., van Es, J. H., Mohammed, S., Heck, A. J., Maurice, M. M., and Clevers, H. (2012) Tumour suppressor RNF43 is a stem-cell E3 ligase that induces endocytosis of Wnt receptors. *Nature* **488**, 665-669
11. Carmon, K. S., Gong, X., Yi, J., Thomas, A., and Liu, Q. (2014) RSPO-LGR4 functions via IQGAP1 to potentiate Wnt signaling. *Proc Natl Acad Sci U S A* **111**, E1221-1229
12. Garcia, M. I., Ghiani, M., Lefort, A., Libert, F., Strollo, S., and Vassart, G. (2009) LGR5 deficiency deregulates Wnt signaling and leads to precocious Paneth cell differentiation in the fetal intestine. *Dev Biol* **331**, 58-67
13. Kinzel, B., Pikiolak, M., Orsini, V., Sprunger, J., Isken, A., Zietzling, S., Desplanches, M., Dubost, V., Breustedt, D., Valdez, R., Liu, D., Theil, D., Muller, M., Dietrich, B., Bouwmeester, T., Ruffner, H., and Tchorz, J. S. (2014) Functional roles of Lgr4 and Lgr5 in embryonic gut, kidney and skin development in mice. *Dev Biol* **390**, 181-190
14. Planas-Paz, L., Orsini, V., Boulter, L., Calabrese, D., Pikiolak, M., Nigsch, F., Xie, Y., Roma, G., Donovan, A., Marti, P., Beckmann, N., Dill, M. T., Carbone, W., Bergling, S., Isken, A., Mueller, M., Kinzel, B., Yang, Y., Mao, X., Nicholson, T. B., Zamponi, R., Capodici, P., Valdez, R., Rivera, D., Loew, A., Ukomadu, C., Terracciano, L. M., Bouwmeester, T., Cong, F., Heim, M. H., Forbes, S. J., Ruffner, H., and Tchorz, J. S.

- (2016) The RSPO-LGR4/5-ZNRF3/RNF43 module controls liver zonation and size. *Nat Cell Biol* **18**, 467-479
15. Walker, F., Zhang, H. H., Odorizzi, A., and Burgess, A. W. (2011) LGR5 Is a Negative Regulator of Tumorigenicity, Antagonizes Wnt Signalling and Regulates Cell Adhesion in Colorectal Cancer Cell Lines. *PLoS One* **6**, e22733
 16. Fukuma, M., Tanese, K., Effendi, K., Yamazaki, K., Masugi, Y., Suda, M., and Sakamoto, M. (2013) Leucine-rich repeat-containing G protein-coupled receptor 5 regulates epithelial cell phenotype and survival of hepatocellular carcinoma cells. *Exp Cell Res* **319**, 113-121
 17. Gong, X., Carmon, K. S., Lin, Q., Thomas, A., Yi, J., and Liu, Q. (2012) LGR6 Is a High Affinity Receptor of R-Spondins and Potentially Functions as a Tumor Suppressor. *PLoS One* **7**, e37137
 18. Snyder, J. C., Rochelle, L. K., Ray, C., Pack, T. F., Bock, C. B., Lubkov, V., Lyerly, H. K., Waggoner, A. S., Barak, L. S., and Caron, M. G. (2017) Inhibiting clathrin-mediated endocytosis of the leucine-rich G protein-coupled Receptor-5 diminishes cell fitness. *J Biol Chem*
 19. Kwon, M. S., Park, B. O., Kim, H. M., and Kim, S. (2013) Leucine-rich repeat-containing G-protein coupled receptor 5/GPR49 activates G12/13-Rho GTPase pathway. *Molecules and cells* **36**, 267-272
 20. Noritake, J., Watanabe, T., Sato, K., Wang, S., and Kaibuchi, K. (2005) IQGAP1: a key regulator of adhesion and migration. *Journal of cell science* **118**, 2085-2092
 21. Johnson, M., Sharma, M., and Henderson, B. R. (2009) IQGAP1 regulation and roles in cancer. *Cell Signal* **21**, 1471-1478
 22. Smith, J. M., Hedman, A. C., and Sacks, D. B. (2015) IQGAPs choreograph cellular signaling from the membrane to the nucleus. *Trends Cell Biol* **25**, 171-184
 23. Hall, A. (2012) Rho family GTPases. *Biochem Soc Trans* **40**, 1378-1382
 24. Noritake, J., Fukata, M., Sato, K., Nakagawa, M., Watanabe, T., Izumi, N., Wang, S., Fukata, Y., and Kaibuchi, K. (2004) Positive role of IQGAP1, an effector of Rac1, in actin-meshwork formation at sites of cell-cell contact. *Mol Biol Cell* **15**, 1065-1076
 25. Li, Z., McNulty, D. E., Marler, K. J., Lim, L., Hall, C., Annan, R. S., and Sacks, D. B. (2005) IQGAP1 promotes neurite outgrowth in a phosphorylation-dependent manner. *J Biol Chem* **280**, 13871-13878
 26. Elliott, S. F., Allen, G., and Timson, D. J. (2012) Biochemical analysis of the interactions of IQGAP1 C-terminal domain with CDC42. *World journal of biological chemistry* **3**, 53-60
 27. Nouri, K., Fansa, E. K., Amin, E., Dvorsky, R., Gremer, L., Willbold, D., Schmitt, L., Timson, D. J., and Ahmadian, M. R. (2016) IQGAP1 Interaction with RHO Family Proteins Revisited: KINETIC AND EQUILIBRIUM EVIDENCE FOR MULTIPLE DISTINCT BINDING SITES. *J Biol Chem* **291**, 26364-26376
 28. Mustata, R. C., Van Loy, T., Lefort, A., Libert, F., Strollo, S., Vassart, G., and Garcia, M. I. (2011) Lgr4 is required for Paneth cell differentiation and maintenance of intestinal stem cells ex vivo. *EMBO Rep*
 29. Sato, T., Vries, R. G., Snippert, H. J., van de Wetering, M., Barker, N., Stange, D. E., van Es, J. H., Abo, A., Kujala, P., Peters, P. J., and Clevers, H. (2009) Single Lgr5 stem cells build crypt-villus structures in vitro without a mesenchymal niche. *Nature* **459**, 262-265
 30. Braut-Boucher, F., Pichon, J., Rat, P., Adolphe, M., Aubery, M., and Font, J. (1995) A non-isotopic, highly sensitive, fluorimetric, cell-cell adhesion microplate assay using calcein AM-labeled lymphocytes. *J Immunol Methods* **178**, 41-51

31. Carmon, K. S., Lin, Q., Gong, X., Thomas, A., and Liu, Q. (2012) LGR5 Interacts and Cointernalizes with Wnt Receptors To Modulate Wnt/beta-Catenin Signaling. *Mol Cell Biol* **32**, 2054-2064
32. Snyder, J. C., Rochelle, L. K., Marion, S., Lyerly, H. K., Barak, L. S., and Caron, M. G. (2015) Lgr4 and Lgr5 drive the formation of long actin-rich cytoneme-like membrane protrusions. *Journal of cell science* **128**, 1230-1240
33. Masuho, I., Ostrovskaya, O., Kramer, G. M., Jones, C. D., Xie, K., and Martemyanov, K. A. (2015) Distinct profiles of functional discrimination among G proteins determine the actions of G protein-coupled receptors. *Sci Signal* **8**, ra123
34. Hollins, B., Kuravi, S., Digby, G. J., and Lambert, N. A. (2009) The c-terminus of GRK3 indicates rapid dissociation of G protein heterotrimers. *Cell Signal* **21**, 1015-1021
35. Masuho, I., Martemyanov, K. A., and Lambert, N. A. (2015) Monitoring G Protein Activation in Cells with BRET. *Methods Mol Biol* **1335**, 107-113
36. Iguchi, T., Sakata, K., Yoshizaki, K., Tago, K., Mizuno, N., and Itoh, H. (2008) Orphan G protein-coupled receptor GPR56 regulates neural progenitor cell migration via a G alpha 12/13 and Rho pathway. *J Biol Chem* **283**, 14469-14478
37. Watanabe, T., Wang, S., and Kaibuchi, K. (2015) IQGAPs as Key Regulators of Actin-cytoskeleton Dynamics. *Cell structure and function* **40**, 69-77
38. White, C. D., Erdemir, H. H., and Sacks, D. B. (2012) IQGAP1 and its binding proteins control diverse biological functions. *Cell Signal* **24**, 826-834
39. Gong, X., Azhdarinia, A., Ghosh, S. C., Xiong, W., An, Z., Liu, Q., and Carmon, K. S. (2016) LGR5-targeted antibody-drug conjugate eradicates gastrointestinal tumors and prevents recurrence. *Mol Cancer Ther* **15**, 1580-1590
40. Zhang, B., Wang, Z. X., and Zheng, Y. (1997) Characterization of the interactions between the small GTPase Cdc42 and its GTPase-activating proteins and putative effectors. Comparison of kinetic properties of Cdc42 binding to the Cdc42-interactive domains. *J Biol Chem* **272**, 21999-22007
41. Grohmanova, K., Schlaepfer, D., Hess, D., Gutierrez, P., Beck, M., and Kroschewski, R. (2004) Phosphorylation of IQGAP1 modulates its binding to Cdc42, revealing a new type of rho-GTPase regulator. *J Biol Chem* **279**, 48495-48504
42. McNulty, D. E., Li, Z., White, C. D., Sacks, D. B., and Annan, R. S. (2011) MAPK scaffold IQGAP1 binds the EGF receptor and modulates its activation. *J Biol Chem* **286**, 15010-15021
43. Barretina, J., Caponigro, G., Stransky, N., Venkatesan, K., Margolin, A. A., Kim, S., Wilson, C. J., Lehar, J., Kryukov, G. V., Sonkin, D., Reddy, A., Liu, M., Murray, L., Berger, M. F., Monahan, J. E., Morais, P., Meltzer, J., Korejwa, A., Jane-Valbuena, J., Mapa, F. A., Thibault, J., Bric-Furlong, E., Raman, P., Shipway, A., Engels, I. H., Cheng, J., Yu, G. K., Yu, J., Aspesi, P., Jr., de Silva, M., Jagtap, K., Jones, M. D., Wang, L., Hatton, C., Palesscandolo, E., Gupta, S., Mahan, S., Sougnez, C., Onofrio, R. C., Liefeld, T., MacConaill, L., Winckler, W., Reich, M., Li, N., Mesirov, J. P., Gabriel, S. B., Getz, G., Ardlie, K., Chan, V., Myer, V. E., Weber, B. L., Porter, J., Warmuth, M., Finan, P., Harris, J. L., Meyerson, M., Golub, T. R., Morrissey, M. P., Sellers, W. R., Schlegel, R., and Garraway, L. A. (2012) The Cancer Cell Line Encyclopedia enables predictive modelling of anticancer drug sensitivity. *Nature* **483**, 603-607
44. Briehner, W. M., and Yap, A. S. (2013) Cadherin junctions and their cytoskeleton(s). *Curr Opin Cell Biol* **25**, 39-46
45. Takaishi, K., Sasaki, T., Kotani, H., Nishioka, H., and Takai, Y. (1997) Regulation of cell-cell adhesion by rac and rho small G proteins in MDCK cells. *J Cell Biol* **139**, 1047-1059
46. Wu, C., Qiu, S., Lu, L., Zou, J., Li, W. F., Wang, O., Zhao, H., Wang, H., Tang, J., Chen, L., Xu, T., Sun, Z., Liao, W., Luo, G., and Lu, X. (2014) RSPO2-LGR5 signaling has tumour-suppressive activity in colorectal cancer. *Nat Commun* **5**, 3149

47. Chen, P. H., Chen, X., Lin, Z., Fang, D., and He, X. (2013) The structural basis of R-spondin recognition by LGR5 and RNF43. *Genes Dev* **27**, 1345-1350
48. Zebisch, M., and Jones, E. Y. (2015) Crystal structure of R-spondin 2 in complex with the ectodomains of its receptors LGR5 and ZNRF3. *J Struct Biol* **191**, 149-155
49. Zebisch, M., and Jones, E. Y. (2015) ZNRF3/RNF43--A direct linkage of extracellular recognition and E3 ligase activity to modulate cell surface signalling. *Progress in biophysics and molecular biology* **118**, 112-118
50. Gao, Y., Kitagawa, K., Hiramatsu, Y., Kikuchi, H., Isobe, T., Shimada, M., Uchida, C., Hattori, T., Oda, T., Nakayama, K., Nakayama, K. I., Tanaka, T., Konno, H., and Kitagawa, M. (2006) Up-regulation of GPR48 induced by down-regulation of p27Kip1 enhances carcinoma cell invasiveness and metastasis. *Cancer Res* **66**, 11623-11631
51. Gong, X., Yi, J., Carmon, K. S., Crumley, C. A., Xiong, W., Thomas, A., Fan, X., Guo, S., An, Z., Chang, J. T., and Liu, Q. J. (2014) Aberrant RSPO3-LGR4 signaling in Keap1-deficient lung adenocarcinomas promotes tumor aggressiveness. *Oncogene*
52. Snyder, J. C., Rochelle, L. K., Lyster, H. K., Caron, M. G., and Barak, L. S. (2013) Constitutive internalization of the leucine-rich G protein-coupled receptor-5 (LGR5) to the trans-Golgi network. *J Biol Chem* **288**, 10286-10297
53. Heuberger, J., and Birchmeier, W. (2010) Interplay of cadherin-mediated cell adhesion and canonical Wnt signaling. *Cold Spring Harbor perspectives in biology* **2**, a002915
54. Fuchs, E., Tumber, T., and Guasch, G. (2004) Socializing with the neighbors: stem cells and their niche. *Cell* **116**, 769-778
55. Sato, T., van Es, J. H., Snippert, H. J., Stange, D. E., Vries, R. G., van den Born, M., Barker, N., Shroyer, N. F., van de Wetering, M., and Clevers, H. (2011) Paneth cells constitute the niche for Lgr5 stem cells in intestinal crypts. *Nature* **469**, 415-418
56. Ritsma, L., Ellenbroek, S. I., Zomer, A., Snippert, H. J., de Sauvage, F. J., Simons, B. D., Clevers, H., and van Rheenen, J. (2014) Intestinal crypt homeostasis revealed at single-stem-cell level by in vivo live imaging. *Nature* **507**, 362-365
57. Phillips, D. R., Jennings, L. K., and Edwards, H. H. (1980) Identification of membrane proteins mediating the interaction of human platelets. *J Cell Biol* **86**, 77-86
58. Schneider, C. A., Rasband, W. S., and Eliceiri, K. W. (2012) NIH Image to ImageJ: 25 years of image analysis. *Nat Methods* **9**, 671-675

Figure Legends

Figure 1. Loss of LGR5 in intestinal crypt organoids resulted in disorganization of F-actin and β -catenin. (A) Bright-field micrographs of wild-type and LGR5-KO mouse intestinal crypt organoids cultured in matrigel. (B) Confocal microscopy images of F-actin (red) in wild-type and LGR5-KO organoids. Nuclei were counterstained using TO-PRO-3 (blue). (C) Quantification of cortical F-actin. (D) Confocal images of β -catenin in WT and LGR5-KO organoids. Nuclei were counterstained using TO-PRO-3 (blue). Arrows included for image reference. (E) Quantification of β -catenin. Error bars are SD (N = 15-20 crypts). ***, P < 0.001 vs WT.

Figure 2. LGR5 overexpression in CHO cells led to increase in cortical F-actin and cell-cell adhesion. (A) Representative confocal images of ICC showing detection of LGR5 on the cell membrane at 4 °C in CHO-LGR5 stable cell line but not in parental CHO cells (a-b), phase contrast images depicting morphological changes resulting from LGR5 overexpression (c-d), and confocal images of F-actin staining with rhodamine-phalloidin (e-f). (B-C) Quantification of cell length (B) and cortical actin (C) of CHO and CHO-LGR5 cells. Error bars are SD (N = 20-30 cells). ***, P < 0.001 vs parental CHO cells. (D) Wound healing assay results of CHO and CHO-LGR5 cells at 8 and 12 hours post wounding. Error bars are SEM (N = 3). *, P < 0.05 vs. control CHO cells. (E) Results of cell-cell adhesion analysis using the Calcein-AM assay. Error bars are SEM (N = 3). **, P < 0.01 vs CHO cells.

Figure 3. Overexpression of LGR5 in HEK293T cells increased cortical F-actin levels. (A) Confocal images of phalloidin staining of HEK293T cells expressing vector control, myc-tagged LGR5 wild-type (LGR5-WT) or LGR5 lacking the C-terminal tail (LGR5 Δ C). (B) Quantification of fluorescence of the lines drawn in (A). (C) Representative WB results of G- and F-actin as separated by the Triton X-100 method. (D) Quantification of F and G actin WB results expressed as ratio of F- vs G-actin. (E) Representative WB results of G- and F-actin of HEK293-vector or -LGR5-WT cells after treatment with RSPO1 (100 ng/ml) or vehicle for overnight. (F). Quantification of WB results of G/F actin. All error bars are SEM (N = 3). *, P < 0.05 compared to vector cells

Figure 4. LGR5 did not exhibit GEF (guanine exchange factor) activity with any of the four heterotrimeric G protein subfamilies. (A) A schematic diagram showing the principle of the BRET assay system. Agonist-bound GPCR exerts GEF activity, leading to the dissociation of inactive heterotrimeric G proteins into active GTP-bound G α and Venus-G $\beta\gamma$ subunits. The free Venus-G $\beta\gamma$ then interacts with the masGRK3ct-Nluc to produce the BRET signal. (B-D) Real-time measurement of GEF activity in living cells. HEK293T/17 cells were transfected with GPCR (dopamine D2 (D2R), M3 acetylcholine (M3R), dopamine D1 (D1R), or bradykinin B2 receptors (BDKRB2), or LGR5), G α subunit (GaoA, G α q, Gas, or G α 13) with the BRET sensor pair, Venus-G $\beta\gamma$ and masGRK3ct-Nluc. Agonists (100 nM dopamine for D1R and D2R, 100 nM acetylcholine for M3R, 100 nM bradykinin for BDKRB2, or 20 nM RSPO3 for LGR4 and LGR5) were applied on transfected cells to stimulate GPCRs at 0 sec. (F) Representative WB results of active RhoA GTPase pulldown assay in stable HEK293T cells overexpressing vector, myc-LGR5, or myc-GPR56. Cells were starved O/N, then treated +/- 10% serum for 15 min. (G) Quantification of WB results of Rho-GTPase. Error bars are SEM (N = 2). *, P < 0.05 compared to vector and LGR5 cells.

Figure 5. LGR5 binds to the C-terminal half of IQGAP1. (A) WB results of Flag-tagged IQGAP1 co-IP with Myc-LGR5-WT, Myc-LGR5 Δ C and membrane-tethered Myc-LGR5 extracellular domain (ECD). (B) WB results of co-IP of endogenous IQGAP1 and LGR5 in LoVo cells. (C) A schematic diagram of IQGAP1 domain structure and the LGR5 binding results of

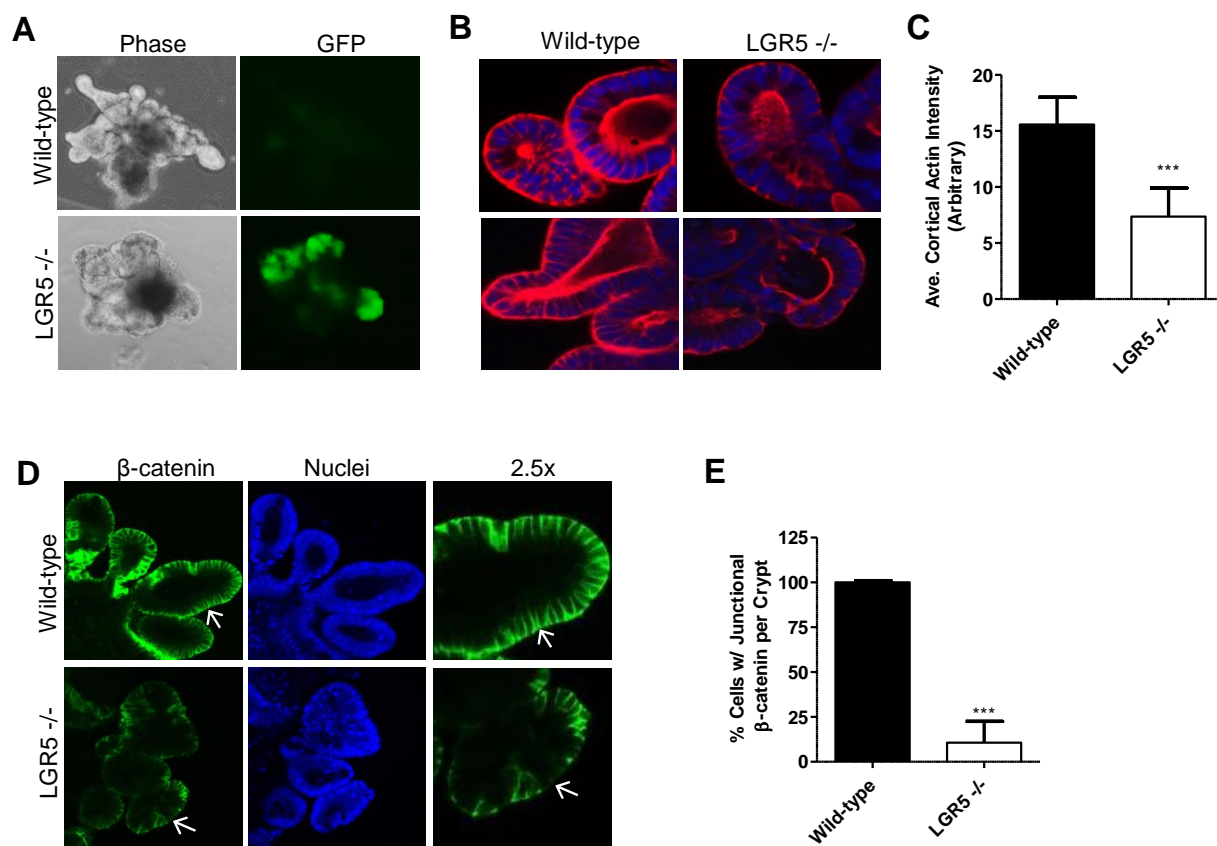
various mutants tested. The domains are: CHD, calponin-homology domain; IR, IQGAP-specific repeat motif; WW, domain with two conserved Trp (W) residues; IQ, calmodulin-binding IQ motif; GRD, RasGAP-related domain, RGCT, Ras GAP C-terminus. The numbers denote the amino acid residues where mutant proteins/deletion regions start and end. (D) WB results of co-IP of Flag-IQGAP1 mutants with LGR5-WT using whole cell lysates. (E) WB results of co-IP of Flag-IQGAP1 C-terminal mutants with Myc-LGR5-WT using whole cell lysates. (F) WB results of co-IP of purified IQGAP1 fragment (DR6, amino acids 877-1558) with LGR5-WT. NS, indicates non-specific (NS) band. Each experiment was repeated 2-3 times and shown here are representative WB results.

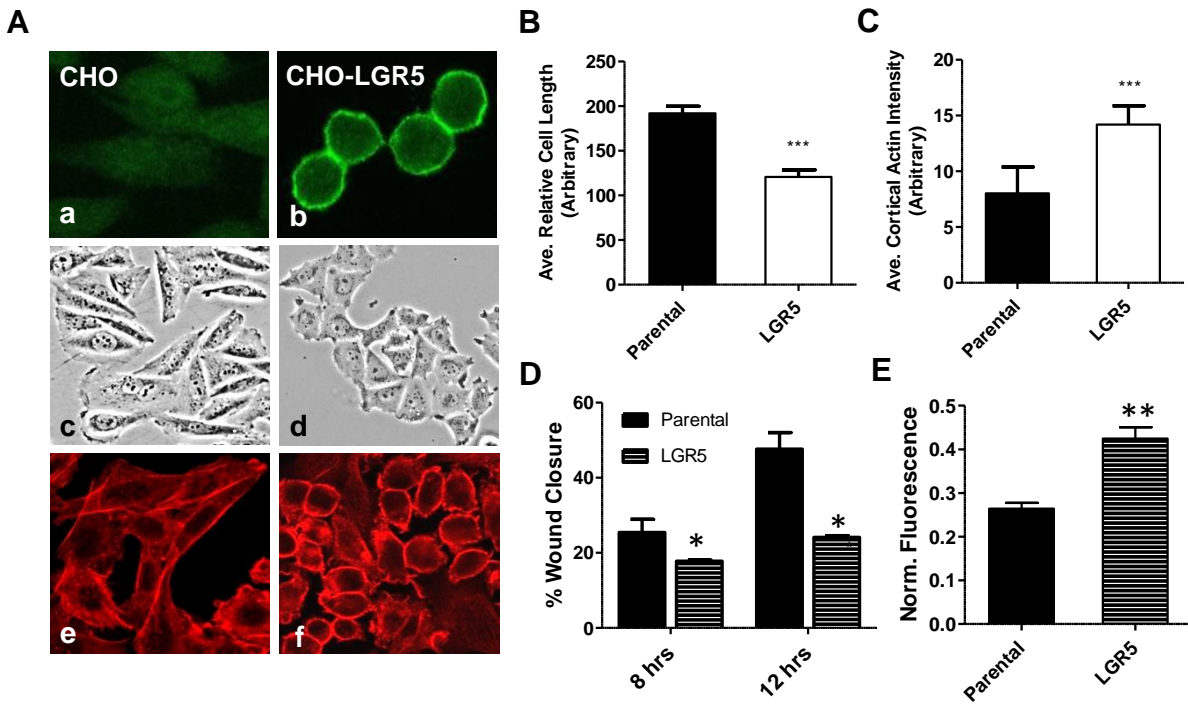
Figure 6. LGR5 increased binding of Rac1 to IQGAP1 via regulating phosphorylation of IQGAP1 at Ser1441/1443. (A) WB results of IQGAP1, Rac1 and actin following IP of IQGAP1 in parental CHO (P) and CHO-LGR5 cells. HC and LC, heavy and light chains of the IP antibody, respectively. (B) WB results of IQGAP1, Rho and CDC42 following IP of IQGAP1. (C) WB of active (GTP bound, binding to PAK1-PBD) and total Rac1. (D) WB results of pSer of IQGAP1 (pSer-IQ1) probed by anti-phosphoserine antibody following IP of IQGAP1 in HEK293 cells overexpressing LGR5 or LGR5 Δ C (lacking C-terminal tail). (E) WB results of pSer, LGR5, actin, and Rac1 following IP of IQGAP1. (F). WB results of pSer of IQGAP1 in HEK293-vector or -LGR5 cells before and after treatment with PMA. Each experiment was repeated 2-3 times and shown here are representative WB results.

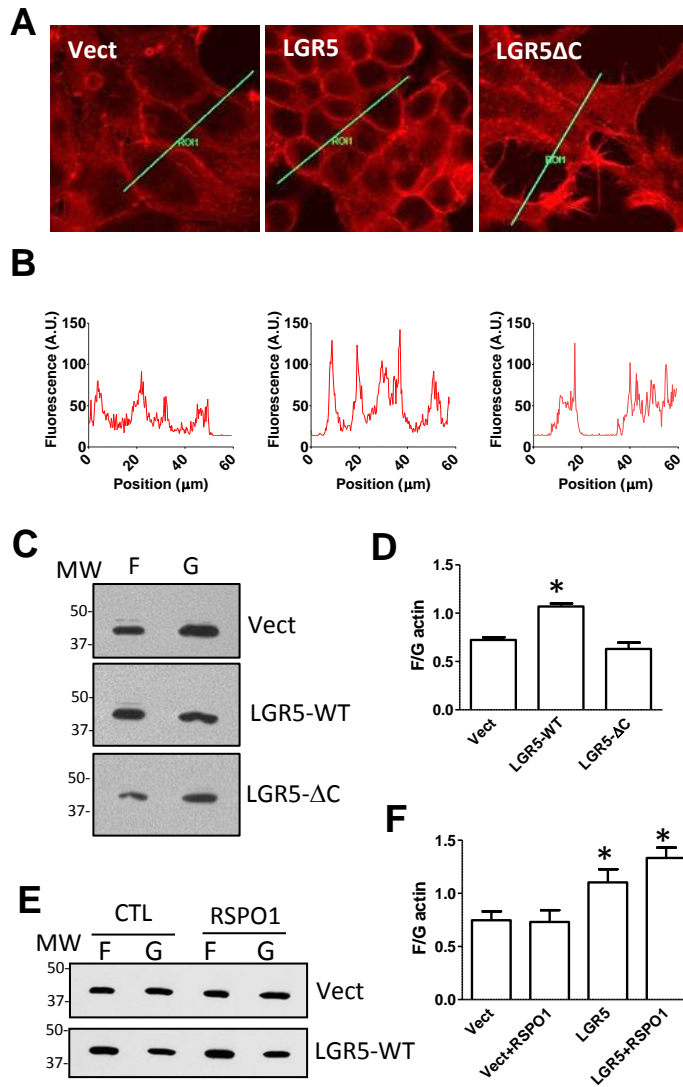
Figure 7. KD of LGR5 in LoVo colon cancer cells altered cytoskeletal structure and decreased the level of membrane associated IQGAP1 and β -catenin. (A) WB results in control and LoVo cells with KD of IQGAP1 or LGR5. (B) Confocal images of LGR5 (green) in control and cells with KD of IQGAP1 or LGR5. F-actin was stained with rhodamine-labeled phalloidin (red). (C) Confocal images of IQGAP1 in control and LoVo cells with KD of LGR5 or IQGAP1. (D) Quantification of membrane-associated IQGAP1. Error bars are SEM (N = 20-30 cells). ***, $P \leq 0.001$ vs. parental and vector cells. (E) Confocal images of β -catenin. (F) Quantification of cytoplasmic β -catenin based on relative signal intensity. Error bars are SEM (N = 20-30 cells). ** and *** are $P \leq 0.01$ and 0.001 compared to parental and vector cells. C and E images are 2.5x magnification compared to B.

Figure 8. KD of LGR5 in LoVo cells resulted in loss of IQGAP1 interaction with Rac1/actin and decreased cell-cell adhesion. (A) Results of Calcein-AM cell-cell adhesion assay. Error bars are SEM (N = 3). *, $P < 0.05$ and **, $P \leq 0.01$ vs controls. (B) Representative WB analysis results of soluble (S) and insoluble (I) E-cadherin in LoVo cells with vector control, KD of LGR5 (shLGR5-89), or KD of IQGAP1 (shIQ1) when extracted at the indicated concentrations of NP-40. (C) Quantification of WB results of E-cadherin. Error bars are SEM (N = 3). *, $P < 0.05$ compared to vector cells. (D) WB results of IQGAP1, actin and Rac1 in control and LoVo cells with KD of LGR5 or IQGAP1. (E) WB of serine phosphorylation of IQGAP1 in LGR5-KD LoVo cells.

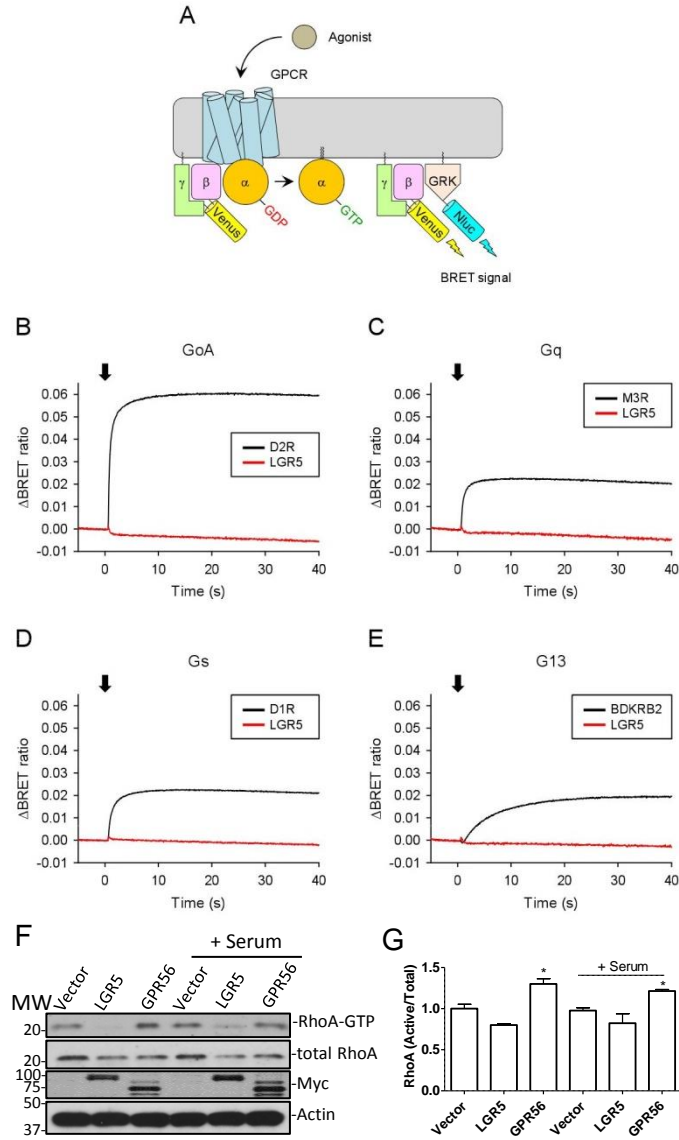
Figure 9. A schematic diagram illustrating the mechanism of LGR5 in the regulation of cell-cell adhesion through the IQGAP1-Rac1 pathway. In the absence of LGR5 (left panel), phosphorylated IQGAP1 is free of Rac1-GTP and can thus bind to β -catenin to disrupt the interaction of β -catenin and α -catenin, leading to separation of the E-cadherin adhesion complex from the actin cytoskeleton and weak cell-cell adhesion. In the presence of LGR5 (right panel), the receptor reduces phosphorylation of IQGAP1 which then binds Rac1-GTP, leading to loss of binding to β -catenin as well as enhanced cross-linking of F-actin. This results in the linkage of E-cadherin adhesion complex to the cytoskeleton and stronger cell-cell adhesion.



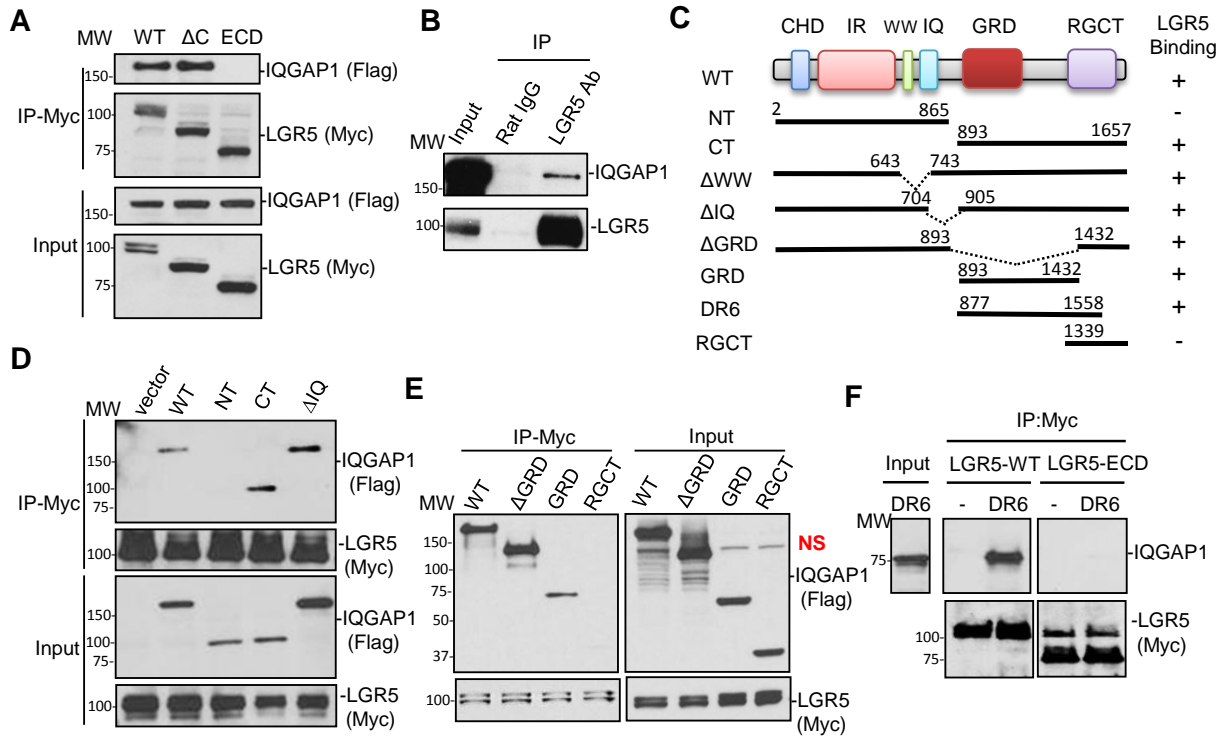


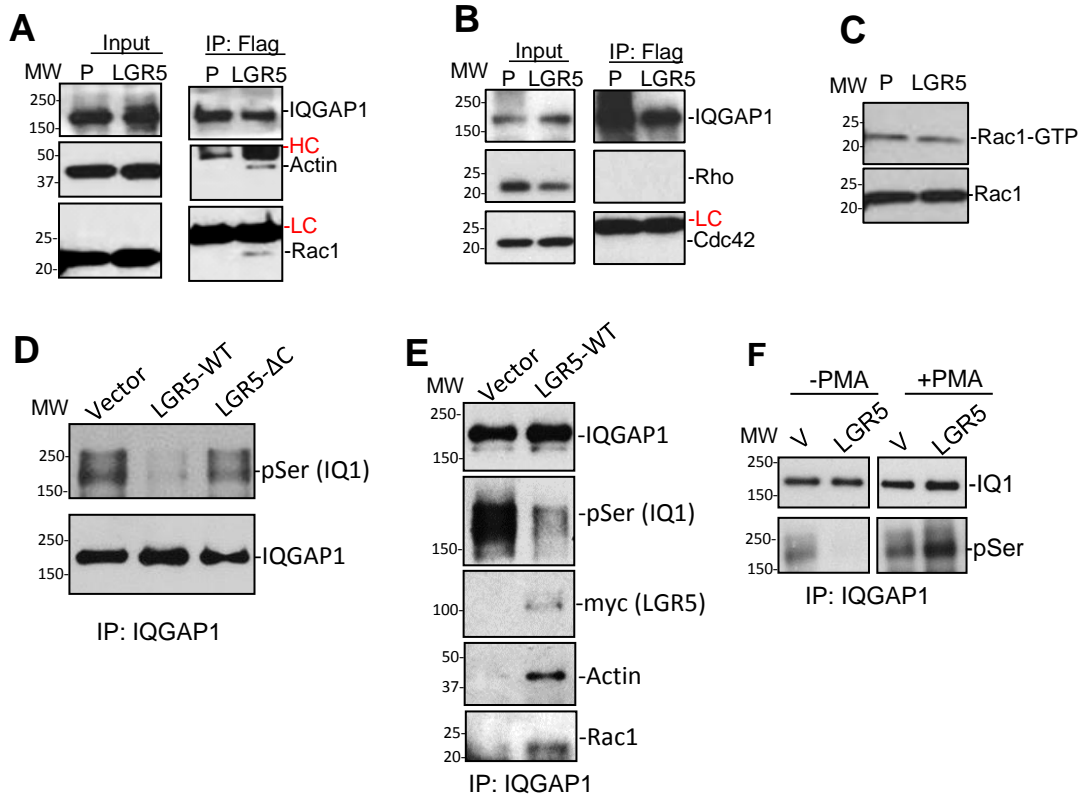


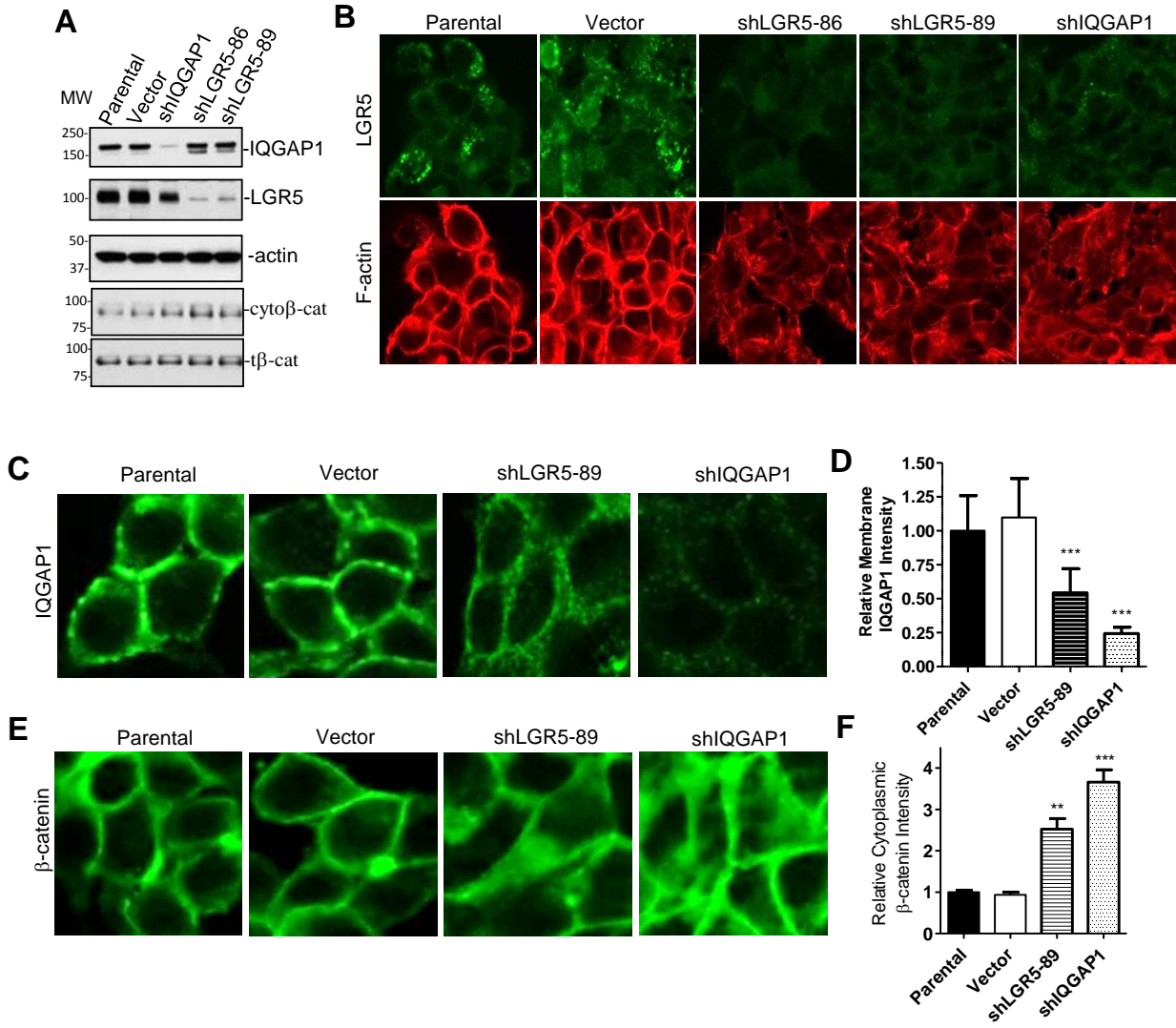
Carmon et al., Figure 4

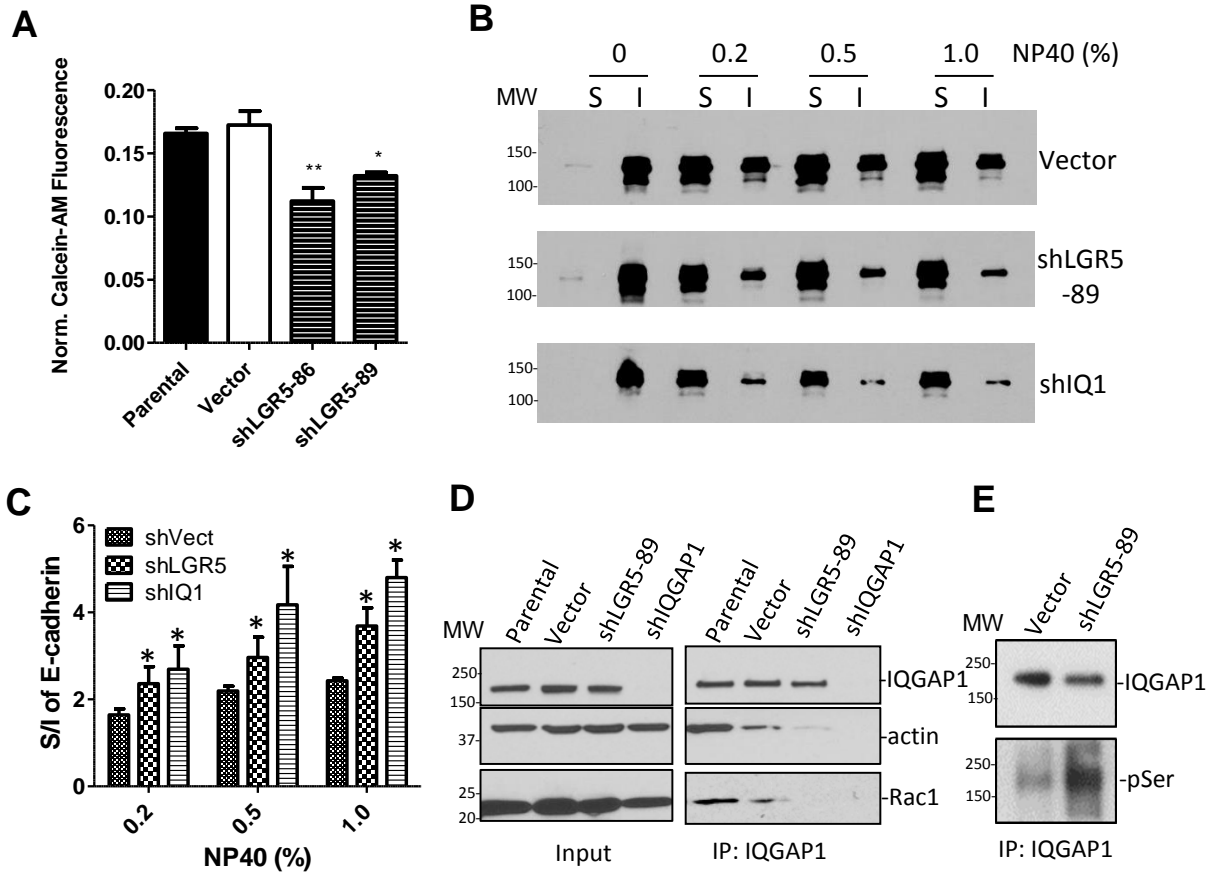


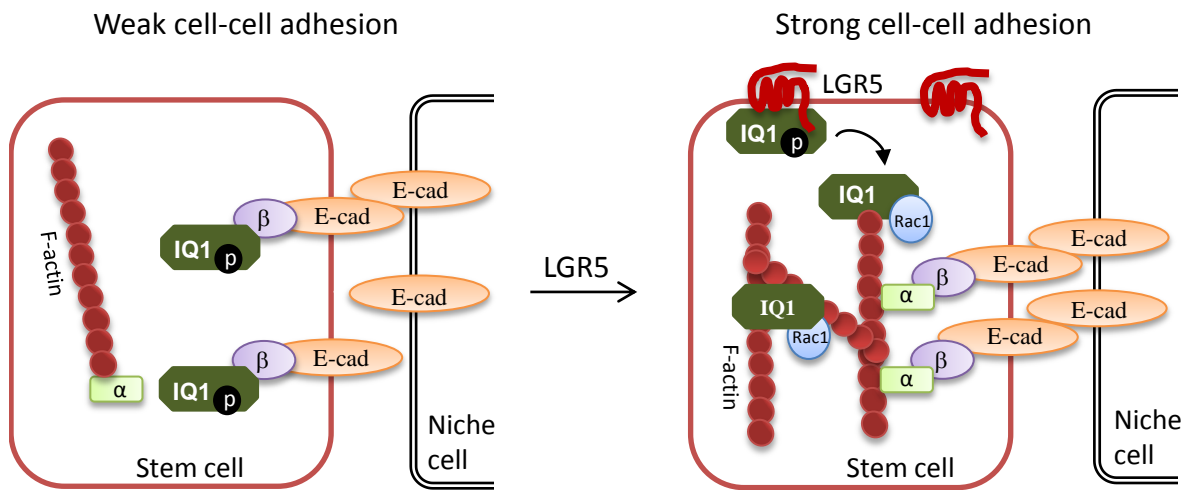
Carmon et al., Figure 5











LGR5 receptor promotes cell-cell adhesion in stem cells and colon cancer cells via the IQGAP1 -Rac1 pathway

Kendra S. Carmon, Xing Gong, Jing Yi, Ling Wu, Anthony Thomas, Catherine M. Moore, Ikuro Masuho, David J. Timson, Kirill A. Martemyanov and Qingyun J. Liu

J. Biol. Chem. published online July 24, 2017

Access the most updated version of this article at doi: [10.1074/jbc.M117.786798](https://doi.org/10.1074/jbc.M117.786798)

Alerts:

- [When this article is cited](#)
- [When a correction for this article is posted](#)

[Click here](#) to choose from all of JBC's e-mail alerts

Supplemental material:

<http://www.jbc.org/content/suppl/2017/07/24/M117.786798.DC1>

This article cites 0 references, 0 of which can be accessed free at <http://www.jbc.org/content/early/2017/07/24/jbc.M117.786798.full.html#ref-list-1>